

Rapid discovery of inhibitors of *Toxoplasma gondii* using hybrid structure-based computational approach

Sandhya Kortagere · Ernest Mui · Rima McLeod · William J. Welsh

Received: 23 December 2010 / Accepted: 16 February 2011 / Published online: 26 February 2011
© Springer Science+Business Media B.V. 2011

Abstract *Toxoplasma (T.) gondii*, the causative agent of toxoplasmosis, is a ubiquitous opportunistic pathogen that infects individuals worldwide, and is a leading cause of severe congenital neurologic and ocular disease in humans. No vaccine to protect humans is available, and hypersensitivity and toxicity limit the use of the few available medicines. Therefore, safer and more effective medicines to treat toxoplasmosis are urgently needed. Using the Hybrid Structure Based (HSB) method, we have previously identified small molecule inhibitors of *P. falciparum* that seem to target a novel protein–protein interaction between the Myosin tail interacting protein and myosin light chain. This pathway has been hypothesized to be involved in invasion of host erythrocytes by the parasite and is broadly conserved among the apicomplexans. Guided by similar computational drug design approaches, we investigated this series of small molecules as potential inhibitors of *T. gondii*. Compound C3-21, identified as the most active inhibitor in this series, exhibited an IC_{50} value ~ 500 nM against *T. gondii*. Among the 16 structural analogs of C3-21 tested thus far, nine additional compounds were identified with IC_{50} values <10.0 μ M. In vitro assays have

revealed that C3-21 markedly limits intracellular growth of *T. gondii* tachyzoites, but has no effect on host cell human foreskin fibroblasts (HFF) at concentrations more than a log greater than the concentration that inhibits the parasites.

Keywords Hybrid structure based method · *Toxoplasma gondii* · Cytotoxicity · Drug design

Introduction

Toxoplasmosis is a clinical problem in persons with immuno-compromising illnesses. Patient classes who are at risk for reactivation of the disease due to *T. gondii* include those undergoing treatment for cancer and auto-immune diseases, and recipients of tissue or organ transplants [1, 2]. Toxoplasmosis also ranks high among diseases that lead to morbidity and death in HIV/AIDS patients, particularly in the developing world. Re-emergence of toxoplasmosis as a life-threatening disease in HIV/AIDS patients is anticipated in the wake of emerging multi-drug resistant strains [3]. *T. gondii* is designated as an NIAID Category B bio-warfare (priority) pathogen [4], in large part due to its danger to both humans and livestock, its persistence in the environment, and the ease with which it disseminates. Taken together, these factors affirm the need for novel, improved medicines to treat and cure toxoplasmosis.

There are only a few medicines that will contain the growth of the tachyzoite stage of the parasite [5–11], and use of these medicines is associated with significant incidences of hypersensitivity (25% of adults) [9] and toxicity [12, 13]. No medicines are available that eliminate encysted, latent bradyzoites [14], which are present in $\sim 30\%$ of the population (~ 2 billion people) worldwide [15].

S. Kortagere · W. J. Welsh (✉)
University of Medicine and Dentistry of New Jersey, Robert
Wood Johnson Medical School, 675 Hoes Lane, Piscataway,
NJ 08854, USA
e-mail: welshwj@umdnj.edu

E. Mui · R. McLeod
The University of Chicago, 5841 South Maryland Avenue,
MC 2114, Room S-206, Chicago, IL 60637, USA

Present Address:
S. Kortagere
Department of Microbiology and Immunology, Drexel
University College of Medicine, Philadelphia, PA 19129, USA

Combined administration of pyrimethamine with either sulfadiazine or clindamycin is currently the treatment of choice for toxoplasmosis. These medicines are active against the tachyzoite form of *T. gondii*, but neither can access, inhibit or kill the bradyzoite form of the parasite present in tissue cysts [16]. *T. gondii*, the causative agent of toxoplasmosis in humans and other warm blooded animals is an obligate intracellular protozoan parasite belonging to the Apicomplexan family [17]. *T. gondii* exists as sporozoites in oocysts, as bradyzoites in cysts and as tachyzoites. Upon contact with a host cell, sporozoites, tachyzoites and bradyzoites can invade within seconds in a process dependent on actin and myosin driven by parasite motility [18]. The actin-myosin machinery is required for invasion and gliding motility among all the Apicomplexan parasites [19]. Previous studies have shown that the actin-myosin complex is localized at the parasite's inner membrane complex (IMC) with other accessory proteins such as GAP45 and GAP50 [20, 21]. Invasion of the epithelial cells appears to be mediated via the conoid, a cone shaped structure on the tachyzoite, where the IMC is interrupted [22, 23]. At this junction the parasite membrane fuses with the plasma membrane of the host cell creating a pathway for entry [23]. Given the absence of this actin—myosin machinery in the human host and its remote homology to host myosin heavy chains, the myosin tail interacting protein (MTIP) in complex with the myosin light chain tail (called Myosin-A) is an attractive drug target [24–27]. Thus we have previously designed small molecule inhibitors against this protein–protein interaction in *P. falciparum* using the hybrid structure based method [28]. Since the myosin motor is well conserved among apicomplexans, it could be also hypothesized to be a unique drug target in *T. gondii*.

The Myosin Light Chain 1, or TgMLC1 [29–31] is the ortholog of MTIP in *T. gondii*. Using the crystal structure of MTIP-MyoA complex in *P. falciparum*, we constructed a hypothetical structure model of the MTIP-MyoA complex in *T. gondii*. This complex was used as an input to the HSB method to screen for small molecule inhibitors of *T. gondii*. In addition, the proposed study also estimated the effect of cytotoxicity of these compounds and hence their validity as lead compounds against *T. gondii* and possibly other apicomplexans.

Materials and methods

Hybrid structure based method

The HSB protocol, described in detail elsewhere [32], was employed for the virtual screening of nearly 3 million compounds to identify small-molecule inhibitors of

T. gondii. The HSB procedure involved 4 major steps, namely: (1) construct a structural model of the *T. gondii* MTIP; (2) design the 3D pharmacophore based on the key molecular interactions between MyoA and MTIP in the complex; (3) screen the in-house molecular libraries to identify “hits”; and (4) re-rank the hits using customized molecular docking and scoring schemes. Subsequent in vitro biological assays including in vitro toxicity studies were conducted on the top hits emanating from this process.

Construction of a structural model of *T. gondii* MTIP and MyoA

In the absence of the X-ray crystal structure for the *T. gondii* MTIP-MyoA complex, homology modeling techniques were employed to build a structural model of the *T. gondii* MTIP-MyoA_tail complex using the published X-ray crystal structure of *Plasmodium* MTIP-MyoA_tail as the template (PDB Entry 2AUC) [21]. This procedure started by aligning the relevant sequences of the corresponding MTIP and MyoA_tail regions of the two proteins. These sequences were aligned using the multiple sequence alignment program CLUSTALW [33]. A three-dimensional model of the *T. gondii* MTIP-MyoA_tail complex was built based upon the high degree of sequence homology between *T. gondii* and *Plasmodium* in these regions (Fig. 1), using the published X-ray crystal structure 2AUC [21] with the homology modeling program Modeller (version 9.0) [34]. Similarly, the MyoA_tail region of *T. gondii* was generated from the structure of MyoA in *P. yoelii* in the MTIP-MyoA crystal structure. The modeled MyoA_tail was manually docked, guided by the pose of the MyoA_tail in the *Plasmodium* MTIP-MyoA crystal structure. Finally, the side chains of the MTIP-MyoA complex of *T. gondii* were energy minimized until convergence was achieved using the default parameterization in AMBER force field (version 9) [35].

Generation of a 3D pharmacophore

The MTIP-MyoA_tail binding region was explored to identify the specific points of interaction between corresponding chemical groups in the MTIP pocket and the MyoA helix (Fig. 2). This procedure yielded a 4-point pharmacophore, which defines the specific 3D geometric arrangement of structural features (chemical atoms/groups) that are responsible for the tight binding between MTIP and MyoA. This analysis was extremely useful, since we utilized the resulting pharmacophore as a pattern to computationally screen an in-house chemical library containing over three million commercially available compounds to identify hits that match these constraints. The combined pharmacophore

A

<i>P. knowlesi</i>	KDMFNTKSSNGKLRIEDASHNARKLGLAPSSIDEKKIRDLYGDSLTQEYQYLEYLTMCVHD
<i>T. gondii</i>	YARFNARASGGKYSTGDAMILARQLGLAPSYADKQAFEEKSGDNLDYASFQKFVGTSTHP
	:*.**: ** **:** :*: :*: **: * :*: :*: **
<i>P. knowlesi</i>	RDNMEELIKMFSHFDNNSGFLTKNQMKNILTTWGDALTEQEANDALNAFSSDRINYKL
<i>T. gondii</i>	EDNIEDLVEAFAYFDVSKHGYLTRKQMGNIIMTYGEPLTTEEFNALAAEYFTSDQIDYRQ
	.***:*.**: **: * :*: ***** ** *: * : * : * : * : * : * : *
<i>P. knowlesi</i>	FCEDIL----
<i>T. gondii</i>	FCKAMLERRE
	** : *

B

Residue#	804	805	806	807	808	809	810	811	812	813	814	815	816
<i>P. yoelii</i>	L	M	R	V	Q	A	H	I	R	K	R	M	V
<i>T. gondii</i>	I	I	R	A	Q	A	H	I	R	R	H	L	V

Fig. 1 **a** Sequence comparison of the MTIP regions of *P. knowlesi* and MLC1 from *T. gondii*. Sequence information was taken from the Apicomplexan Database (<http://apidb.org/apidb/>). Residues colored in red represent those amino acids that form the binding pocket for the MyoA_tail helix in *P. knowlesi* (PDB entry 2AUC) [21]. Symbols: asterisk means identity; colon means high similarity; and dot means

similarity. **b** Sequence comparison of the corresponding MyoA_tail regions of *P. yoelii* and *T. gondii*. This 13-residue sequence was obtained from the *Plasmodium* crystal structure (PDB entry 2AUC) [21]. Residues colored in red were used for the generation of the 4-point pharmacophore

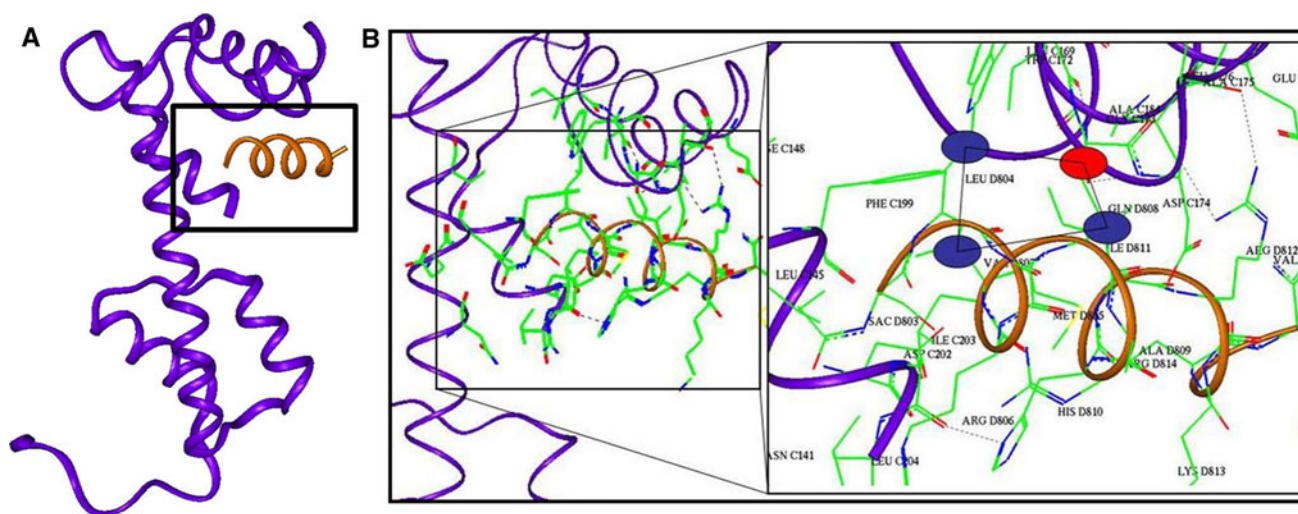


Fig. 2 **a** MTIP-MyoA_tail interaction in *T. gondii* model depicts the helical MyoA_tail (orange ribbons) binding within a deep groove of MTIP (blue ribbons). **b** Image depicting interaction region for *T. gondii* MTIP (blue backbone, green sidechains) and the MyoA

tail (amber helix). Inset at far right shows more detailed, close-up image of the binding pocket and key interactions between MTIP and MyoA. Our 4-point pharmacophore comprises residues Gln808 (red oval, hydrophilic), Leu804, Val807 and Ile811 (blue ovals, hydrophobic)

was used to screen the molecular libraries using UNITY module of Sybyl (version 7.1, Tripos Inc) to identify hits.

The resulting 150 hits were then docked in the MTIP binding groove using the “docking & scoring” program GOLD (version 3.1) [36], which were then ranked using GoldScore, Chemscore and a customized scoring scheme to identify 60 best ranking hits [28, 32]. The customized scoring scheme was developed based on the interactions of

the ligands with MTIP. A complete description of the method is available from Kortagere and Welsh [32]. Briefly, the method consists of deriving the information about all the interacting pairs of atoms between the ligand and the protein binding site residues that are within a specified cutoff distance. A contact score weight w_i was assigned to each of the ligand i docked into the protein such that:

$$\sum_{i=1}^N w_i = 1 \quad (1)$$

the customized docking score of an active compound j with i conformations was derived as.

$$S_{i,j} = w_i s_{ij} \quad (2)$$

where s_{ij} was the Goldscore for the compound j in its i th conformation. Further, similar calculations were performed by replacing Goldscore with Chemscore. Finally, the consensus score for compound j was computed as:

$$S_{\max,j} = \max(S_{i,\text{goldscore}}, S_{i,\text{chemscore}}) \quad (3)$$

The 60 best ranking compounds ranked by the consensus scoring scheme were filtered with respect to LogP, MW, and other *Lipinski Rule of 5* criteria (ChemAxon®) to yield a final ranked subset of 25 compounds which were purchased and tested in inhibition assays against *T. gondii* to assess their in vitro inhibitory activity.

Parasite inhibition assays

Four-day old confluent cultures of human foreskin fibroblasts (HFF), cultured in 96-well plates, were infected with 2.0×10^3 tachyzoites of RH strain of *T. gondii* per well and cultured for 1 h to allow parasite invasion. Inhibitors were added and cells cultured for 3 days. They were then supplemented with ^3H uracil and cultured overnight, allowing for uracil incorporation into cells and thus parasite growth to be assessed by liquid scintillation counting [37]. Absence of toxicity for mammalian host cells was demonstrated first by visual inspection of the monolayer and in separate ^3H thymidine incorporation assays by non-confluent cell monolayers.

Results and discussion

Modeling the MTIP-MyoA interactions and inhibitor discovery

The parasite *T. gondii* exists in three forms: oocysts, bradyzoites and tachyzoites and may remain dormant until it comes into contact with the right type of host cell. Upon contact with a host cell, these parasites can invade within seconds in a process dependent on actin and myosin driven by parasite motility [18]. Uniquely, the invasive machinery employed by *T. gondii* and other apicomplexan parasites for entering and leaving all host cells (insect, animal, human) involves a critical interaction between two proteins: the MyoA_tail, and MTIP. Our design strategy was

to develop a small-molecule competitive inhibitor that disrupts the formation of the protein–protein complex between MTIP and MyoA. Specifically, the inhibitors would block the binding of the α -helix of the MyoA_tail in the MTIP binding pocket of *T. gondii*. The published X-ray crystal structure of the MTIP-MyoA complex in *Plasmodium* (PDB code: 2AUC) [21] enabled us to implement our HSB strategy [32] that integrates ligand-based and structure-based drug design approaches. Since the crystal structure for the *T. gondii* MTIP-MyoA complex was not available during the present study, homology modeling techniques were used to build a structural model of the *T. gondii* MTIP-MyoA_tail complex. This was made possible because sequence comparison between *P. knowlesi* and *T. gondii* for the MTIP protein revealed a high degree of conservation (identity is 80% overall and 85% in the MTIP binding groove) between the two species (Fig. 1a), while sequence alignment of the corresponding MyoA_tail regions revealed 54% identity and 100% similarity (Fig. 1b). However, it is worth noting that the published X-ray crystal structure of the *Plasmodium* MTIP-MyoA complex [2AUC] is composed of two highly similar, but distinct, *Plasmodium* species: MTIP from *P. knowlesi*, and MyoA from *P. yoelii* [21]. Superposition of the backbone atoms of our *T. gondii* structural model and the *Plasmodium* crystal structure showed a modest root mean squared deviation (rmsd) of 1.27 Å.

The 17 residues of *Plasmodium* MTIP interacting with the MyoA_tail were highly conserved, including Phe-149, Leu-169, Leu-176, and Phe-199 which were totally identical in the sequenced *Plasmodium* and *Toxoplasma* MTIPs. Using this structural information for MTIP and MyoA, a four point pharmacophore was developed based on the interaction of the modeled MyoA tail with modeled MTIP structure of *T. gondii*. One hundred and fifty molecules were initially identified by screening the Shape Signatures databases using the 4-point pharmacophore as a query to the UNITY program (Fig. 2). These hits were docked into the binding site of MTIP of *T. gondii* and the docked complexes were ranked using consensus scoring function to identify the 60 best ranking compounds. Further, these compounds were then filtered through ADMET filters to identify the 25 best ranking drug-like compounds. The in silico screening, docking and scoring of 150 compounds takes about 2 hours on a quad core dual linux processor with an operating system of Red Hat enterprise linux (ver 5), hence justifying the rapidness of the approach.

Results from the in vitro inhibition assay in which tachyzoites of *T. gondii* type 1 strain were incubated before and after challenge with 10 compounds are shown in Fig. 3a. Each compound was tested in triplicate. Comparison of the rank order of the 10 test compounds between

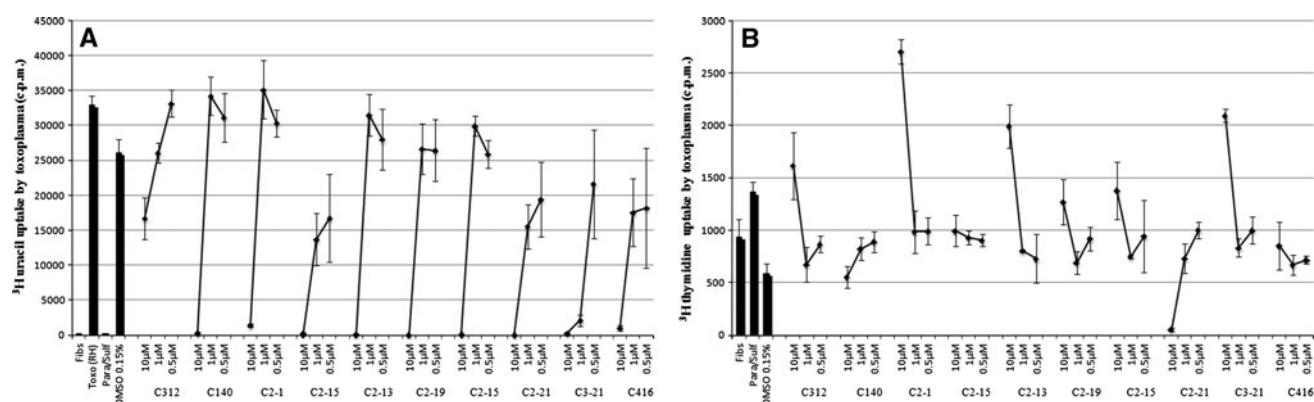


Fig. 3 **a** Inhibition of *T. gondii* tachyzoites by various compounds (shown along X-axis with # compound number), measured as diminished uptake of tritiated uracil c.p.m.* 10^3 (Y-axis). Results from three different concentrations (10, 1 and 0.5 μM) of the compounds

are reported. **b** Results from cytotoxicity assays for the primary set of 10 compounds are shown. No compounds, except 10 μM of compound 16, were toxic to the host cell using a ^3H thymidine assay

their experimental values and computational predictions (Table 1) revealed good agreement (correlation coefficient $r^2 = 0.84$). Among the 10 structural analogs of C3-21 tested, we have found IC_{50} values $< 10.0 \mu\text{M}$ for 9 compounds and $< 5.0 \mu\text{M}$ for 4 compounds (Fig. 4a).

Insights from predicted C3-21 interactions with MTIP

Inspection of C3-21 docked inside the MTIP ligand binding pocket (Fig. 5) revealed several probable key interactions shared by the *T. gondii* MyoA_{tail}. C3-21 was oriented such that R1 was largely solvent exposed; R2 and R4 blocked the opening of the binding pocket; and R3 extended deep inside (8–9 Å) the binding cleft to engage in specific hydrophobic and hydrophilic contacts. These insights provided valuable clues in making appropriate choices for substituents R1, R2, R3, and R4 to identify the second generation of C3-21 like compounds. Specifically, we chose sterically compact hydrophilic groups at R1 (e.g., $-\text{C}(\text{O})-\text{OCH}_3$, $-\text{CH}_2\text{OH}$, $-\text{OCH}_3$, $-\text{CH}_2\text{NH}_2$, and $-\text{CH}_2\text{N}(\text{Me})_2$); and aromatic groups at R2 and R4 substituted with hydrophobes $-\text{Me}$, $-\text{Et}$, $-\text{Pr}$, $-\text{t-Bu}$, $-\text{F}$, $-\text{Cl}$, and $-\text{Br}$ alone or in combination at the ortho and para positions. Finally, R3 was chosen to mimic MyoA's hydrophobic tail (Leu804, Val807, Ile811) and strongly basic Arg812 that together filled the binding cleft. Based on this choice of functional groups, six candidate molecules were synthesized and screened using the inhibition assay described above. The results are shown in Fig. 4a. In this set of compounds, C3-20 performed significantly better than the parent compound in the parasite inhibition assay against *T. gondii*.

Further, in vitro cytotoxicity studies of C3-21 and its analogs were performed using host human foreskin fibroblasts (HFF). The results from the study showed no evidence of toxicity in these cells despite exposure and incubation with the compounds for 4 days with a

concentration at least 1.5 logs greater than the IC_{50} (see Figs. 3b, 4b).

Comparison of activities of compounds between *T. gondii* and *P. falciparum*

All the compounds described in this study were initially assessed against *P. falciparum* [28]. The MTIP and MyoA complex was first discovered in *P. falciparum* and was shown to be a key component of the parasite invasion machinery. The components of the invasion machinery have been hypothesized to be conserved among all members of the Apicomplexan family [20, 22]. Interestingly, C3-21 has an IC_{50} value of 500 nM against *T. gondii* and 385 nM against *P. falciparum*. A similar trend was observed with C3-20 that has an IC_{50} of ~ 400 nM against *T. gondii* and 300 nM against *P. falciparum*. Previously, we have shown that C3-21 inhibited the gliding motility of *P. berghei* sporozoites in a dose dependent manner [28]. Given the similar levels of efficacy in both *T. gondii* and *P. falciparum*, we hypothesized that both C3-20 and C3-21 must be inhibiting the parasites through a similar mechanism of action involving MTIP. Among the other compounds, C416 and C2-1 were potent inhibitors of *P. falciparum* with IC_{50} values of 145 and 47 nM respectively. However, both these compounds inhibited *T. gondii* with IC_{50} values between 4 and 10 μM , suggesting they probably work through other targets.

Conclusions

The present study has led to the discovery of C3-21 as a lead compound, with an $\text{IC}_{50} < 500$ nM against *T. gondii*. Among the 16 structural analogs of C3-21 tested thus far, we have found 4 compounds with $\text{IC}_{50} < 5.0 \mu\text{M}$ and 9

Table 1 Predicted ranking of compounds using HSB method and their corresponding IC₉₀ and IC₅₀ values are reported

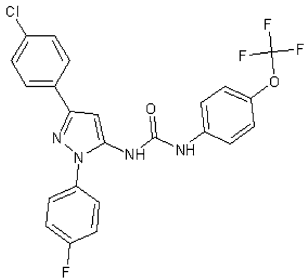
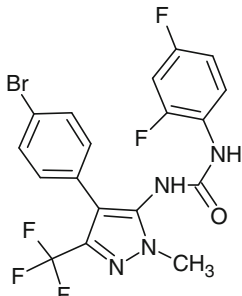
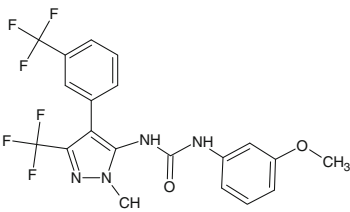
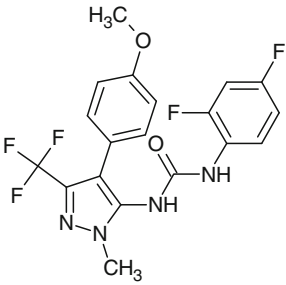
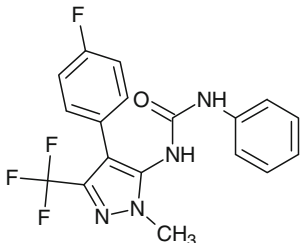
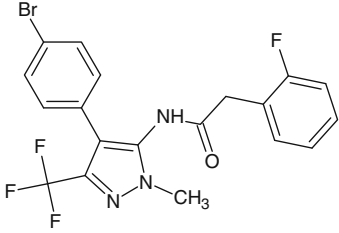
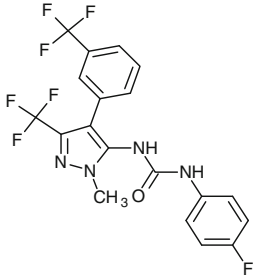
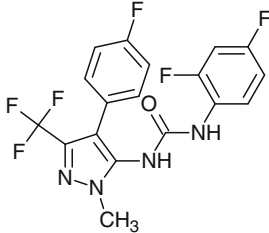
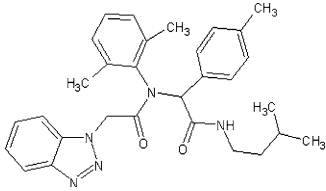
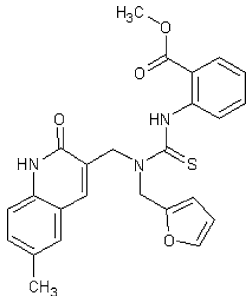
Compound	HSB ranking	Expt. ranking	IC ₉₀ (μM)	IC ₅₀ (μM)	Toxicity ^a
C3-21	1	1	≤0.75	<0.5	>10
					
C2-12	2	3	<10 ^b	<10	<10
					
C2-15	3	2	<5	~1	>10
					
C416	4	4	10 > n > 1 ⁺	10 > n > 1	>10
					
C2-19	5	5	10 > n > 1	10 > n > 1	>10
					

Table 1 continued

Compound	HSB ranking	Expt. ranking	IC ₉₀ (μM)	IC ₅₀ (μM)	Toxicity ^a
C2-1	6	9	10 > n > 1	10 > n > 1	>10
					
C2-21	7	6	10 > n > 1	10 > n > 1	>10
					
C2-13	8	7	10 > n > 1	10 > n > 1	>10
					
C140	9	8	10 > n > 1	10 > n > 1	>10
					
C312	10	10	>10	≥10	>10
					

⁺ 10 > n > 1 denotes the value to be between 10 and 1 μM, less than 10 but greater than 1; 10 and 1 μM were the concentrations tested

^a Toxicity determined using highest tested concentration of compound (10 μM) on host cells compared with 0.15% DMSO (v/v) control

^b Toxic to host cells at this concentration

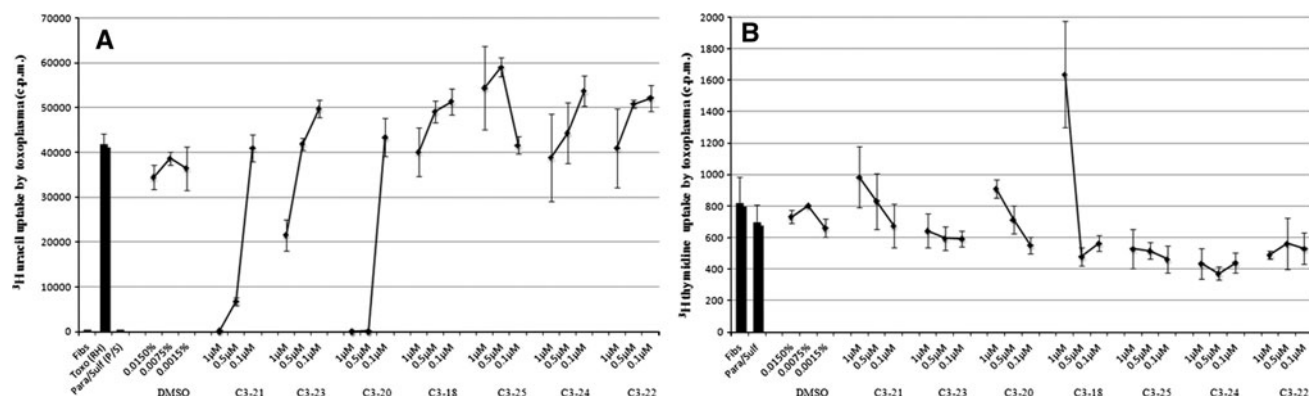
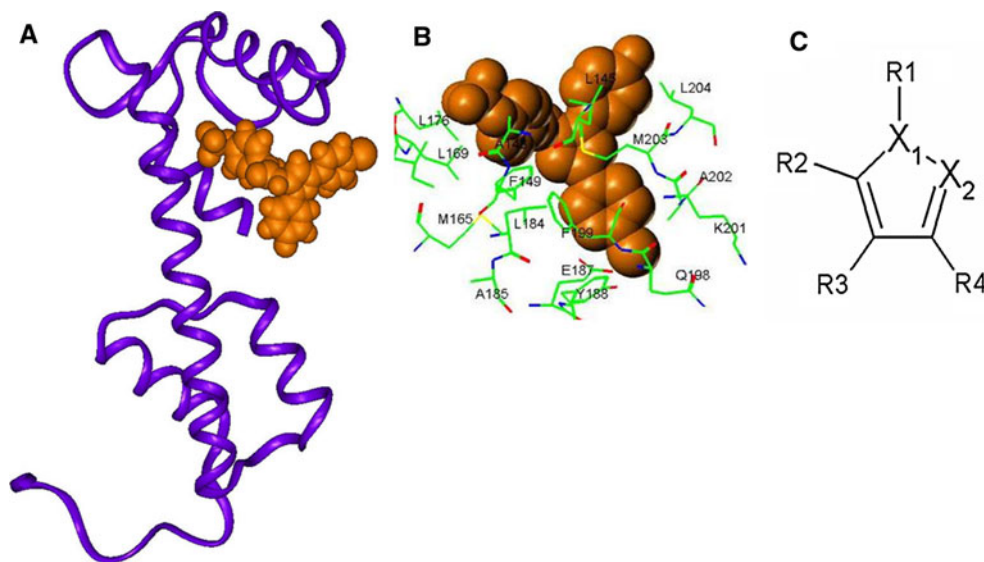


Fig. 4 **a** Inhibition of *T. gondii* tachyzoites by analogs of compound C3-21 measured as diminished uptake of tritiated uracil (Y-axis). Results from three different concentrations (1, 0.5 and 0.1 μM) of the compounds are reported. **b** All analogs of compound C3-21 (shown

along X-axis with compound number and measured in 3 different concentrations namely 1, 0.5 and 0.1 μM) showed no evidence of toxicity on human HFF host cells, measured as uptake of tritiated thymidine c.p.m.*10³(Y-axis)

Fig. 5 **a** C3-21 computationally docked inside the MTIP binding pocket. C3-21 is rendered in orange space-filling mode, while MTIP is shown as blue ribbons. **b** Close-up view of C3-21 (in orange space fill mode) in the binding site of MTIP. Interacting residues from MTIP are shown in stick mode and colored atom type (C-green, O-red, S-yellow, N-blue) **c** Drawing of C3-21 core structure and substitution pattern (R1–R4) which is optimized for tight binding within the MTIP binding pocket. X1 and X2 can be C, N, O, S



compounds with IC₅₀ < 10.0 μM. C3-21 and its analogs were selected to target the MTIP binding pocket, thereby acting as competitive inhibitors of the MTIP MyoA_{tail} interaction. In vitro assays have revealed that C3-21 markedly limits invasion and thus subsequent intracellular growth of *T. gondii* tachyzoites, but has no effect on host cell human foreskin fibroblasts (HFF) at concentrations more than a log greater than the concentration that inhibits the parasites. Interestingly, C3-20 and C3-21 have nearly similar IC₅₀ values against *T. gondii* and *P. falciparum* and may be working through similar mechanism that warrant consideration as broad spectrum inhibitors of apicomplexan parasites. Further studies are planned to validate their target and mechanism of action as starting points for the development of therapeutic inhibitors of *T. gondii*.

Acknowledgments This work was funded in part by grant NIH R21-GM081394 to WJW from the National Institute of General Medical Sciences. Funding for this research was also provided to WJW by U.S. Army Small Business Innovation Research (SBIR) program contract W81XWH-04-C-0024. This research project was also made possible by a grant that was awarded by the Center for Military Biomaterial Research (CeMBR) of Rutgers University and administered by the US Army Medical Research and Materiel Command (USAMRMC) and the Telemedicine & Advanced Technology Research Center (TATRC), Fort Detrick, Maryland 21702, under Contract Number: W81XWH-04-2-0031. This work was also funded by the NIH-NIAID (Grant #R43AI078763) to RM and WJW. The views, opinions and findings contained in this research are those of the participating laboratories and do not necessarily reflect the views of the Department of Defense and should not be construed as an official DoD/Army policy unless so designated by other documentation. No official endorsement should be made. We thank Dr. Sean Ekins for thoughtful discussions.

References

1. Michaels MG, Wald ER, Fricker FJ, del Nido PJ, Armitage J (1992) Toxoplasmosis in pediatric recipients of heart transplants. *Clin Infect Dis* 14:847–851
2. Peacock JE Jr, Greven CM, Cruz JM, Hurd DD (1995) Reactivation toxoplasmic retinochoroiditis in patients undergoing bone marrow transplantation: is there a role for chemoprophylaxis? *Bone Marrow Transplant* 15:983–987
3. Alfonzo M, Blanc D, Troadec C, Huerre M, Eliasiewicz M et al (2002) Temporary restoration of immune response against *Toxoplasma gondii* in HIV-infected individuals after HAART, as studied in the hu-PBMC-SCID mouse model. *Clin Exp Immunol* 129:411–419
4. Anonymous (2003) NIAID Biodefense research agenda for category B and C priority pathogens. In: NIAID (eds), National Institutes of Health
5. Boyer KM, Holfels E, Roizen N, Swisher C, Mack D et al (2005) Risk factors for *Toxoplasma gondii* infection in mothers of infants with congenital toxoplasmosis: implications for prenatal management and screening. *Am J Obstet Gynecol* 192:564–571
6. Brezin AP, Thulliez P, Couvreur J, Nobre R, McLeod R et al (2003) Ophthalmic outcomes after prenatal and postnatal treatment of congenital toxoplasmosis. *Am J Ophthalmol* 135:779–784
7. Glasner PD, Silveira C, Kruszon-Moran D, Martins MC, Burnier Junior M et al (1992) An unusually high prevalence of ocular toxoplasmosis in southern Brazil. *Am J Ophthalmol* 114:136–144
8. McLeod R, Khan AR, Noble GA, Latkany P, Jalbrzikowski J et al (2006) Severe sulfadiazine hypersensitivity in a child with reactivated congenital *Toxoplasmic chorioretinitis*. *Pediatr Infect Dis J* 25:270–272
9. Roberts F, Mets MB, Ferguson DJ, O'Grady R, O'Grady C et al (2001) Histopathological features of ocular toxoplasmosis in the fetus and infant. *Arch Ophthalmol* 119:51–58
10. Roberts F, Roberts CW, Ferguson DJ, McLeod R (2000) Inhibition of nitric oxide production exacerbates chronic ocular toxoplasmosis. *Parasite Immunol* 22:1–5
11. Roizen N, Kasza K, Karrison T, Mets M, Noble AG et al (2006) Impact of visual impairment on measures of cognitive function for children with congenital toxoplasmosis: implications for compensatory intervention strategies. *Pediatrics* 118:e379–e390
12. Mui EJ, Schiehsler GA, Milhous WK, Hsu H, Roberts CW et al (2008) Novel Triazine JPC-2067-B inhibits *Toxoplasma gondii* in vitro and in vivo. *PLoS Negl Trop Dis* 2:e190
13. Choquet-Kastylevsky G, Vial T, Descotes J (2002) Allergic adverse reactions to sulfonamides. *Curr Allergy Asthma Rep* 2:16–25
14. Bosch J, Turley S, Roach CM, Daly TM, Bergman LW et al (2007) The closed MTIP-myosin a-tail complex from the malaria parasite invasion machinery. *J Mol Biol* 372:77–88
15. Boyer K, Marcink J, McLeod R (2008) *Toxoplasma gondii* (Toxoplasmosis). In: Long S, Proeber CLP (eds) Principles and practice of paediatric infectious diseases, 3rd edn. Churchill Livingstone, New York, pp 1267–1287
16. Nordquist BC, Aronson LR (2008) Pyogranulomatous cystitis associated with *Toxoplasma gondii* infection in a cat after renal transplantation. *J Am Vet Med Assoc* 232:1010–1012
17. Carruthers VB (2002) Host cell invasion by the opportunistic pathogen *Toxoplasma gondii*. *Acta Trop* 81:111–122
18. Striepen B, Jordan CN, Reiff S, van Dooren GG (2007) Building the perfect parasite: cell division in apicomplexa. *PLoS Pathog* 3:e78
19. Baum J, Richard D, Healer J, Rug M, Krnajska Z et al (2006) A conserved molecular motor drives cell invasion and gliding motility across malaria life cycle stages and other apicomplexan parasites. *J Biol Chem* 281:5197–5208
20. Kappe SH, Buscaglia CA, Bergman LW, Coppens I, Nussenzweig V (2004) Apicomplexan gliding motility and host cell invasion: overhauling the motor model. *Trends Parasitol* 20:13–16
21. Bosch J, Turley S, Daly TM, Bogh SM, Villasmil ML et al (2006) Structure of the MTIP-MyoA complex, a key component of the malaria parasite invasion motor. *Proc Natl Acad Sci USA* 103:4852–4857
22. Gubbels MJ, Wieffer M, Striepen B (2004) Fluorescent protein tagging in *Toxoplasma gondii*: identification of a novel inner membrane complex component conserved among Apicomplexa. *Mol Biochem Parasitol* 137:99–110
23. Hu K, Mann T, Striepen B, Beckers CJ, Roos DS et al (2002) Daughter cell assembly in the protozoan parasite *Toxoplasma gondii*. *Mol Biol Cell* 13:593–606
24. Allen ML, Dobrowolski JM, Muller H, Sibley LD, Mansour TE (1997) Cloning and characterization of actin depolymerizing factor from *Toxoplasma gondii*. *Mol Biochem Parasitol* 88:43–52
25. Dobrowolski JM, Niesman IR, Sibley LD (1997) Actin in the parasite *Toxoplasma gondii* is encoded by a single copy gene, ACT1 and exists primarily in a globular form. *Cell Motil Cytoskeleton* 37:253–262
26. Dobrowolski JM, Carruthers VB, Sibley LD (1997) Participation of myosin in gliding motility and host cell invasion by *Toxoplasma gondii*. *Mol Microbiol* 26:163–173
27. Dobrowolski JM, Sibley LD (1996) Toxoplasma invasion of mammalian cells is powered by the actin cytoskeleton of the parasite. *Cell* 84:933–939
28. Kortagere S, Welsh WJ, Morrissey JM, Daly T, Ejigiri I et al (2010) Structure-based design of novel small-molecule inhibitors of *Plasmodium falciparum*. *J Chem Inf Model* 50:840–849
29. Gaskins E, Gilk S, DeVore N, Mann T, Ward G et al (2004) Identification of the membrane receptor of a class XIV myosin in *Toxoplasma gondii*. *J Cell Biol* 165:383–393
30. Heintzelman MB, Schwartzman JD (2001) Myosin diversity in Apicomplexa. *J Parasitol* 87:429–432
31. Meissner M, Schluter D, Soldati D (2002) Role of *Toxoplasma gondii* myosin A in powering parasite gliding and host cell invasion. *Science* 298:837–840
32. Kortagere S, Welsh WJ (2006) Development and application of hybrid structure based method for efficient screening of ligands binding to G-protein coupled receptors. *J Comput Aided Mol Des* 20:789–802
33. Thompson JD, Higgins DG, Gibson TJ (1994) CLUSTAL W: improving the sensitivity of progressive multiple sequence alignment through sequence weighting, position-specific gap penalties and weight matrix choice. *Nucleic Acids Res* 22:4673–4680
34. Sali A, Potterton L, Yuan F, van Vlijmen H, Karplus M (1995) Evaluation of comparative protein modeling by MODELLER. *Proteins* 23:318–326
35. Pearlman DA, Case DA, Caldwell JW, Ross WR, Cheatham TEI et al (1995) AMBER, a package of computer programs for applying molecular mechanics, normal mode analysis molecular dynamics and free energy calculations to simulate the structural and energetic properties of molecules. *Comp Phys Commun* 91:1
36. Jones G, Willett P, Glen RC, Leach AR, Taylor R (1997) Development and validation of a genetic algorithm for flexible docking. *J Mol Biol* 267:727–748
37. Mui EJ, Jacobus D, Milhous WK, Schiehsler G, Hsu H et al (2005) Triazine Inhibits *Toxoplasma gondii* tachyzoites in vitro and in vivo. *Antimicrob Agents Chemother* 49:3463–3467